EXTERNAL HEAT TRANSFER IN INFILTRATED GRANULAR BEDS.

1. ANALYSIS OF A THEORETICAL MODEL

V. A. Borodulya, Yu. S. Teplitskii,
and I. I. Markevich

UDC 66.096.5

A model is proposed for external heat transfer in infiltrated fixed granular beds. The model is analyzed to derive simple equations for calculation of the heat-transfer coefficient.

Heat transfer in infiltrated fixed granular beds is of considerable practical interest in connection with problems of chemical engineering, the drying of dispersed materials, heat treatment of parts in layers of a dispersed heat-transfer agent, rock thermophysics, power engineering, and many other subjects. It therefore continually draws the attention of investigators [1-7].

Several models have been proposed to describe heat transfer in such systems. These models can be tentatively divided into two groups: one-zone models [1, 3, 5, 6], presuming constant porosity over the entire bed of dispersed material; two-zone models, which include a high-porosity zone near the heat-transfer surface [2, 4, 7]. It should be noted that the existing schemes are based on key assumptions which are not always justified. This shortcoming is due to the lack of a general physical theory of disperse systems. On the other hand, there are also no adequately substantiated, simple, and reliable engineering methods of calculating heat transfer in such systems which could indicate the conditions under which different models of heat transfer could be used. The two-zone model proposed here for steady-state heat transfer between a surface and an infiltrated disperse bed is analyzed in just such a context.

The model (Fig. 1) is based on the following assumptions: 1) heat is removed from the bed by the filtered gas; 2) the conductive component of heat flow in the direction of the gas flow is ignored; 3) a gas film of the effective thickness $l_0 = md$* is located near the heat-transfer surface; 4) the thermal conductivity of the gas film (in the direction normal to the heat-transfer surface) is taken as the sum of the conductive and convective components: $\lambda_f = \lambda_f^c + nc_f\rho_f ud/\varepsilon_0$.

The mathematical formulation of the problem of steady-state heat transfer between a surface and infiltrated disperse bed has the form:

plane surface

$$\frac{\partial^2\theta_f}{\partial\xi^2} - \mathrm{Pe}\frac{\lambda}{\varepsilon_0}\frac{\partial\theta_f}{\partial\eta} = 0, \quad 0 \leqslant \xi < \xi_0$$
$$\frac{\partial^2\theta_s}{\partial\xi^2} - \mathrm{Pe}\frac{\partial\theta_s}{\partial\eta} = 0, \quad \xi_0 < \xi \leqslant 1, \tag{1}$$

with the boundary conditions

$$\theta_f(\eta, 0) = 1; \ \theta_f(0, \xi) = \theta_s(0, \xi) = 0; \ \frac{\partial\theta_s(\eta, 1)}{\partial\xi} = 0;$$
$$\frac{\partial\theta_f(\eta, \xi_0)}{\partial\xi} = \lambda\frac{\partial\theta_s(\eta, \xi_0)}{\partial\xi}; \ \theta_f(\eta, \xi_0) = \theta_s(\eta, \xi_0); \tag{2}$$

*It was shown in [7, 8] that with a specified temperature of the heat-transfer surface, the presence of the high-porosity zone can be accounted for by introducing a third-order boundary condition if this zone has a high thermal resistance.

A. V. Lykov Institute of Heat and Mass Transfer, Academy of Sciences of the Belorussian SSR, Minsk. Translated from Inzhenerno-Fizicheskii Zhurnal, Vol. 53, No. 4, pp. 580-585, October, 1987. Original article submitted August 12, 1986.

0022-0841/87/5304-1145$12.50

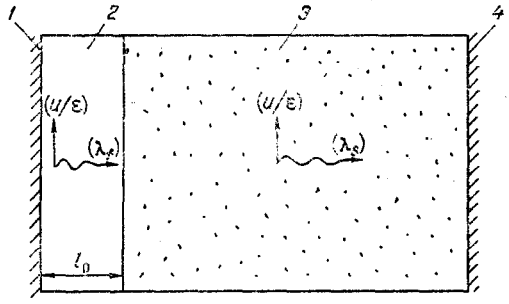

Fig. 1. Heat-transfer model: 1) heat-transfer surface; 2) gas film; 3) disperse infiltrated bed; 4) wall of unit.

cylindrical surface

$$\frac{\partial^2\theta_f}{\partial\xi^2}+\frac{1}{\xi}\frac{\partial\theta_f}{\partial\xi}-\mathrm{Pe}\frac{\lambda}{\varepsilon_0}\frac{\partial\theta_f}{\partial\eta}=0,\ \xi_a\leqslant\xi<\xi_a+\xi_0,$$
$$\frac{\partial^2\theta_s}{\partial\xi^2}+\frac{1}{\xi}\frac{\partial\theta_s}{\partial\xi}-\mathrm{Pe}\frac{\partial\theta_s}{\partial\eta}=0,\ \ \xi_a+\xi_0<\xi\leqslant 1, \tag{3}$$

with the boundary conditions

$$\theta_f(\eta,\ \xi_a)=1;\ \theta_f(0,\ \xi)=\theta_s(0,\ \xi)=0;\frac{\partial\theta_s(\eta,\ 1)}{\partial\xi}=0;$$
$$\frac{\partial\theta_f(\eta,\ \xi_a+\xi_0)}{\partial\xi}=\lambda\frac{\partial\theta_s(\eta,\ \xi_a+\xi_0)}{\partial\xi};\ \ \theta_f(\eta,\ \xi_a+\xi_0)=\theta_s(\eta,\ \xi_a+\xi_0). \tag{4}$$

As can be seen from Eqs. (1)-(4), the dimensionless temperatures in both zones are functions of the following parameters: Pe, λ, ε_0, ξ_0 (plane surface); Pe, λ, ε_0, ξ_0, ξ_a (cylindrical surface). To determine the thermal conductivity and the thickness of the gas interlayer, we used formulas from [9-11], respectively:

$$\lambda_f=\lambda_f^c+0{,}0061\rho_f c_f u d,$$
$$\lambda_s=\lambda_s^0+0{,}1\rho_f c_f u d, \tag{5}$$
$$l_0=0{,}1d.$$

Systems (1)-(2) and (3)-(4) were solved numerically by the establishment method, with the use of a stable implicit finite-difference scheme [12]. The solution allowed us to determine the temperature field in both zones and then calculate the heat-transfer coefficients:

average

$$\overline{\mathrm{Nu}}_{\mathrm{tot}}=\frac{\bar{q}d}{\lambda_f}\Big/\frac{\overline{T}-T_0}{\ln\dfrac{T_w-T_0}{T_w-\overline{T}}};\ \overline{\mathrm{Nu}}_1=\frac{\bar{q}d}{\lambda_f}\Big/(T_w-T_0);$$
$$\overline{\mathrm{Nu}}_2=\frac{\bar{q}d}{\lambda_f}\Big/(T_w-\overline{T_s(x,\ R)}); \tag{6}$$

local

$$\mathrm{Nu}_3=\frac{qd}{\lambda_f}\Big/(T_w-T_0);\ \ \mathrm{Nu}_4=\frac{qd}{\lambda_f}\Big/(T_w-T_s(x,\ R)), \tag{7}$$

where the heat flux q was found from the formulas

$$q=-\frac{\lambda_f(T_w-T_0)}{R}\frac{\partial\theta_f(\eta,\ 0)}{\partial\xi}$$

for the plane surface and

$$q=-\frac{\lambda_f(T_w-T_0)}{R}\frac{\partial\theta_f(\eta,\ \xi_a)}{\partial\xi} \tag{8}$$

for the cylindrical surface.

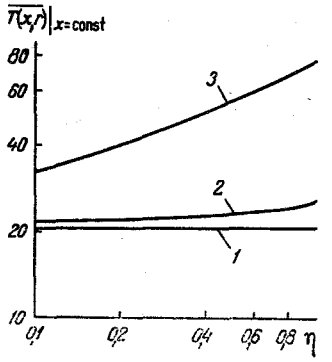

Fig. 2. Dependence of the temperature averaged over the cross section η = const on the dimensionless longitudinal coordinate: 1) Pe = 3158; 2) 31.6; 3) 1.05 (T_w = 100°C; T_0 = 20°C; $\xi_0 = 1.17 \cdot 10^{-3}$; ξ_a = 0.1; λ = 4.62).

We determined the mean values $\bar{q}$ by integrating Eq. (8), and we similarly calculated the mean temperatures T and $\overline{T_s(x, R)}$.

Figures 2-4 show profiles of temperature averaged over the cross section η = const and the local and mean heat-transfer coefficients. It was established that at Pe > 100, the temperature $\overline{T_s(x, r)}/_{x=\text{const}}$ is nearly independent of the longitudinal coordinate (Fig. 2). In accordance with this, at Pe > 100 the heat-transfer coefficients found from the different formulas nearly coincide (Figs. 3 and 4). Appreciable nonuniformity of the temperature $\overline{T_s(x, r)}/_{x=\text{const}}$ develops along the longitudinal coordinate at small Pe (see Fig. 2), so a difference appears between the heat-transfer coefficients calculated from the above formulas (Figs. 3 and 4). An increase in Pe is also accompanied by convergence of the heat-transfer coefficients for the plane and cylindrical surfaces, with these coefficients coinciding at Pe > 500 (ξ_a = 0.1) and Pe > 100 (ξ_a = 0.3).

Equations (1) and (3) can be simplified considerably if we do not take into account the change in temperatures along the longitudinal coordinate and examine the problem of heat transfer in a unidimensional formulation:

for the plane surface

$$\frac{d^2\theta_f}{d\xi^2} - \mathrm{Pe}\frac{\lambda}{\varepsilon_0}\theta_f = 0, \quad 0 \leqslant \xi < \xi_0, \tag{9}$$

$$\frac{d^2\theta_s}{d\xi^2} - \mathrm{Pe}\,\theta_s = 0, \quad \xi_0 < \xi \leqslant 1; \tag{10}$$

$$\theta_f(0) = 1; \quad \frac{d\theta_s(1)}{d\xi} = 0; \quad \frac{d\theta_f(\xi_0)}{d\xi} = \lambda\frac{d\theta_s(\xi_0)}{d\xi} \quad \theta_f(\xi_0) = \theta_s(\xi_0);$$

for the cylindrical surface

$$\frac{d^2\theta_f}{d\xi^2} + \frac{1}{\xi}\frac{d\theta_f}{d\xi} - \mathrm{Pe}\frac{\lambda}{\varepsilon_0}\theta_f = 0, \quad \xi_a \leqslant \xi < \xi_a + \xi_0, \tag{11}$$

$$\frac{d^2\theta_s}{d\xi^2} + \frac{1}{\xi}\frac{d\theta_s}{d\xi} - \mathrm{Pe}\,\theta_s = 0, \quad \xi_a + \xi_0 < \xi \leqslant 1;$$

$$\theta_f(\xi_a) = 1; \quad \frac{d\theta_s(1)}{d\xi} = 0; \quad \frac{d\theta_f(\xi_a + \xi_0)}{a\xi} = \lambda\frac{d\theta_s(\xi_a + \xi_0)}{d\xi}, \tag{12}$$

$$\theta_f(\xi_a + \xi_0) = \theta_s(\xi_a + \xi_0).$$

As can be seen, the change from Eqs. (1)-(4) to unidimensional equations (9)-(12) is made by means of the substitutions $\partial\theta_f/\partial\eta \to \theta_f$ and $\partial\theta_s/\partial\eta \to \theta_s$ and is obviously valid at high values of Pe, when $\partial\theta/\partial\xi \gg \partial\theta/\partial\eta$.

The external heat-transfer coefficient in the unidimensional case is determined by the relations

$$\mathrm{Nu} = \frac{d}{T_s(R) - T_w}\frac{dT_f(0)}{dy} \tag{13}$$

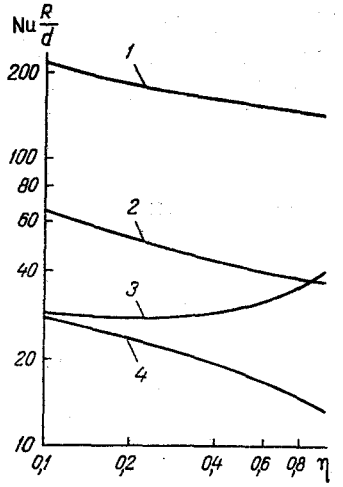

Fig. 3. Dependence of the local heat-transfer coefficients on the dimensionless longitudinal coordinate: 1) Nu_3, Nu_4 (Pe = 3158); 2) Nu_3, Nu_4 (Pe = 31.6); 3, 4) Nu_4 and Nu_3 (Pe = 1.05); $\xi_0 = 1.17 \cdot 10^{-3}$; ξ_α = = 0.1; $\lambda = 4.62$.

(plane surface),

$$\mathrm{Nu} = \frac{d}{T_s(R) - T_w} \frac{dT_f(a)}{dr} \tag{14}$$

(cylindrical surface).

Equations (9), (10) and (11), (12) are easily solved analytically. This allows us to establish the following expressions for the dimensionless heat-transfer coefficients:

plane surface:

$$\mathrm{Nu} = \frac{d}{R} \cdot \frac{(f-\lambda s)(e^{2s-(s+f)\xi_0} - e^{(s+f)\xi_0}) + (f+\lambda s)(e^{(s-f)\xi_0} - e^{2s-(s-f)\xi_0})}{4e^s - 2\mathrm{ch}\, f\xi_0 (e^{2s-s\xi_0} + e^{s\xi_0}) - \frac{2\lambda s}{f} \mathrm{sh}\, f\xi_0 (e^{2s-s\xi_0} - e^{s\xi_0})}; \tag{15}$$

cylindrical surface

$$\mathrm{Nu} = \frac{d}{R} fs\xi^* \frac{I_1(f\xi_\alpha) C_1 - K_1(f\xi_\alpha) C_2}{1 - s\xi^* C}, \tag{16}$$

where $\xi^* = \xi_\alpha + \xi_0$; $C_1 = \lambda S\gamma + f\gamma_0$; $C_2 = \lambda S\beta + f\beta_0$; $C = \lambda S[I_0(f\xi_\alpha)\gamma + K_0(f\xi_\alpha)\beta] + f[I_0(f\xi_\alpha) - \gamma_0 + K_0(f\xi_\alpha)\beta_0]$; $\gamma = -I_1(s)K_1(s\xi^*)K_0(f\xi^*) + K_1(s)I_1(s\xi^*)K_0(f\xi^*)$; $\gamma_0 = I_1(s)K_0(s\xi^*)K_1(f\xi^*) + K_1(s)I_0(s\xi^*)K_1(fs^*)$; $\beta = I_1(s)K_1(s\xi^*)I_0(f\xi^*) - K_1(s)I_1(s\xi^*)I_0(f\xi^*)$; $\beta_0 = I_1(s)K_0(s\xi^*)I_1(f\xi^*) + K_1(s)I_0(s\xi^*)I_1(f\xi^*)$.

For high values of Pe at which the unidimensional approximation is also valid, Eqs. (15) and (16) are simplified considerably and take the form:

$$\mathrm{Nu} = \frac{d}{R} \frac{\lambda s + f^2\xi_0}{1 + \lambda s\xi_0} \tag{15'}$$

(plane surface),

$$\mathrm{Nu} = \frac{d}{R} \frac{\lambda s + f^2\xi_0/K^*}{1 + \lambda\xi_0 sK^*} K^* \tag{16'}$$

(cylindrical surface) ($K^* = K_1(s\xi^*)/K_0(s\xi^*)$).

It should be noted that at $K^* \to 1$ (flat heat exchanger), Eq. (16') changes into Eq. (15'). Equations (15') and (16') show that heat transfer in a fixed infiltrated bed is determined by the thermal resistance both of the gas film and of the disperse bed itself. The rate of heat transfer on the cylindrical sensor also depends on its diameter.

Figure 4 shows curves constructed from Eqs. (15')-(16'). It can be seen that for large Pe, the heat-transfer coefficients calculated from two-dimensional model (1)-(4) and unidimensional formulas (15) and (16) nearly coincide (at Pe > 500 for the plane surface and Pe >

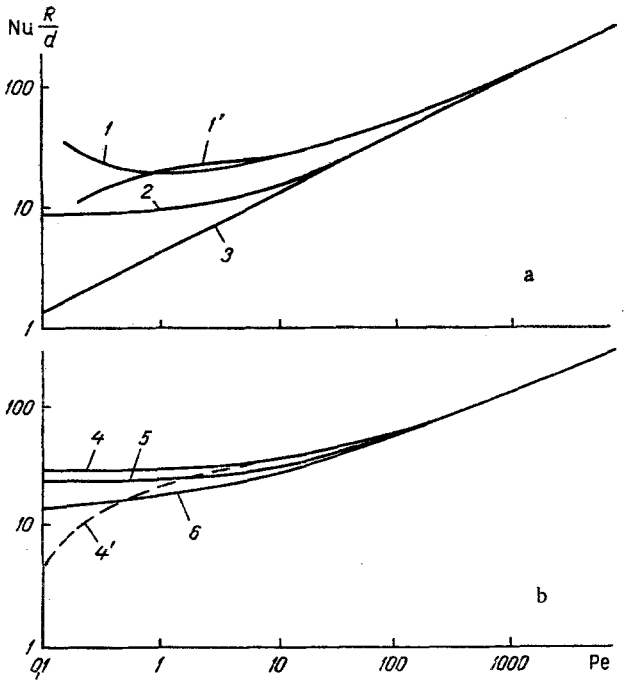

Fig. 4. Dependence of the dimensionless heat-transfer coefficients on the number Pe (T_w = 100°C; T_0 = 20°C; $\xi_0 = 1.17 \cdot 10^{-3}$; λ = 4.62): 1, 1') $\overline{Nu_2}$ and Nu_{tot} from the two-dimensional model; 2) Nu from (15); 3) Nu from (15'); 4, 4') $\overline{Nu_2}$ and $\overline{Nu_{tot}}$ from the two-dimensional model; 5) Nu from (16); 6) Nu from (16'); a) plane heat-transfer surface; b) cylindrical heat-transfer surface (ξ_a = 0.1).

100 for the cylindrical surface). The results of calculations with "exact" formulas (15) and (16) coincide with the results from approximate formulas (15') and (16') at Pe > 10 and Pe > 100 for the plane and cylindrical surfaces, respectively. The cases Pe > 500 for plane heat-transfer surfaces and Pe > 100 for cylindrical surfaces embrace a fairly broad range of practically important systems with a fixed infiltrated bed of solid particles, and experimental data on heat transfer in these cases can be analyzed on the basis of Eqs. (15') and (16').

NOTATION

a, radius of cylindrical heat-transfer surface; c, heat capacity; d, particle diameter; $f = \sqrt{Pe\lambda/\varepsilon_0}$; H, length of heat-transfer surface; I_0, I_1, modified 0-th and first order Bessel functions of the first kind; K_0, K_1, modified 0-th and first order Bessel functions of the second kind (MacDonald functions); m, n, dimensionless coefficients; l_0, thickness of the gas film; q, heat flux; r, y, transverse coordinates for the plane and cylindrical problems; R, width (or radius) of the disperse bed; $s = \sqrt{Pe}$; T, temperature; T_0, temperature of incoming gas; $\overline{T}$, mean (for two zones) temperature at the outlet (x = H); u, filtration velocity; x, longitudinal coordinate (coincident with the direction of the gas flow); α, heat-transfer coefficient; ε_0, porosity of bed; $\xi = y/R$ (plane); $\xi = r/R$ (cylinder); $\xi_a = a/R$; $\xi_0 = l_0/R$; $\eta = x/H$; $\theta = (T - T_0)/(T_w - T_0)$, dimensionless temperature; $\lambda = \lambda_s/\lambda_f$; λ_f^c, molecular thermal conductivity of the gas; λ^0_s, effective thermal conductivity of the disperse bed at u = 0; ρ, density; $Pe = c_f\rho_f u R^2/(H\lambda_s)$, Peclet number; $Nu = \alpha d/\lambda_f$, Nusselt number. Indices: f, gas; s, particles; w, heat-transfer surface.

LITERATURE CITED

1. M. E. Aerov, O. M. Todes, and D. A. Narinskii, Units with a Fixed Granular Bed [in Russian], Leningrad (1979).
2. V. A. Mukhin and N. N. Smirnova, "Study of heat and mass transfer processes in filtration in porous media," Preprint, Institute of Thermophysics, Siberian Branch, Academy of Sciences of the USSR, Novosibirsk (1978), pp. 27-78.
3. J. D. Gabor, Chem. Eng. Sci., 25, 979-984 (1970).
4. J. S. M. Botterill and A. O. O. Denloye, Chem. Eng. Sci., 33, 509-515 (1978).

5. N. V. Antonishin, M. A. Geller, and V. I. Ivanyutenko, Inzh.-Fiz. Zh., 43, No. 3, 360-364 (1982).
6. Yu. A. Buevich and D. A. Kazenin, Zh. Prikl. Mekh. Tekh. Fiz., No. 5, 94-102 (1977).
7. Yu. A. Buevich and E. B. Perminov, Inzh.-Fiz. Zh., 48, No. 1, 35-44 (1985).
8. A. P. Baskakov, B. V. Berg, A. F. Ryzhakov, et al., Heat and Mass Transfer Processes in a Fluidized Bed [in Russian], Moscow (1978).
9. V. A. Borodulya, V. L. Ganzha, Yu. S. Teplitskii, et al., Inzh.-Fiz. Zh., 49, No. 4, 621-626 (1985).
10. N. I. Helperin and V. G. Einstein, Fluidization [in Russian], Moscow (1974), pp. 414-474.
11. V. A. Borodulya, V. L. Ganzha, and V. I. Kovenskii, Hydrodynamics and Heat Transfer in a Fluidized Bed Under Pressure [in Russian], Minsk (1982).
12. A. A. Samarskii and E. S. Nikolaev, Methods of Solving Network Equations [in Russian], Moscow (1978).

EXPERIMENTAL STUDY OF THE TRANSIENT REGIME IN A THERMOPILE WITH ADDITIONAL HEAT REMOVAL

M. E. Babin, V. P. Bezruchko, and V. N. Kozlyuk

UDC 621.396.6.017.72

Experiments have shown that additional heat removal makes it possible to eliminate overheating of the leg of a thermopile and significantly increase the speed of its response. A description is given of the experimental method used.

It was shown in [1] that the use of additional removal of heat from the lateral surface of the leg of a thermopile makes it possible to improve the dynamic characteristics of the latter.

The thermal scheme of a thermopile may be modified differently than in [1], such as by removing heat from the cross section of the leg [2]. Some results of study of such thermopiles were reported in [3].

Here, we generalize results of an experimental study of a transient in cooling thermopiles both with additional heat removal from the cross section and with the conventional design (with heat removal only from the end of the leg). In making the test thermocouples, we used legs with a current height of 4.6 and 8 mm and a diameter of 3 and 2 mm.

The results reported here were obtained from testing thermopiles consisting of several thermocouples. This is in contrast to those studies in [4, 5], which consisted of a single thermocouple.

The unit used in the tests consisted of the radiators of the hot junctions 1, two thermopiles 2, and the object being cooled 3. The cooled object was a copper plate. The heat capacity of the plate was roughly five times greater than the heat capacity of the switching elements. Flowing water served as the heat carrier in the radiators and in the additional cooling device 4.

Temperature was measured with copper—constantin thermocouples attached to the center of mass of the cooled object I, to the heat-absorbing II and heat-emitting III junctions, to the additional cooling device or to a point corresponding to its position in a conventional thermopile, and to two points over the height of the leg V.

The measurement thermocouples on the junctions and in the additional cooling element were soldered in an opening having a diameter twice as great as the diameter d of the thermocouple electrode, while the measurement thermocouple of the leg was glued into a hole having a depth equal to roughly half the cross section of the leg. The diameter of the electrode

---

Institute of Engineering Thermophysics, Academy of Sciences of the Ukrainian SSR, Kiev.
Translated from Inzhenerno-Fizicheskii Zhurnal, Vol. 53, No. 4, pp. 586-589, October, 1987. Original article submitted June 12, 1986.

 0022-0841/87/5304-1150$12.50